

**Ionic conductivity and the mixed alkali effect in  $\text{Li}_x\text{Rb}_{1-x}\text{PO}_3$  glasses**C. Karlsson,<sup>1</sup> A. Mandanici,<sup>2</sup> A. Matic,<sup>1</sup> J. Swenson,<sup>1</sup> and L. Börjesson<sup>1</sup><sup>1</sup>*Department of Applied Physics, Chalmers University of Technology, SE-412 96 Göteborg, Sweden*<sup>2</sup>*Dipartimento di Fisica and INFN, Università di Messina, Sal. Sperone 31, 98166 Messina, Italy*

(Received 16 October 2002; revised manuscript received 14 May 2003; published 8 August 2003)

The temperature and frequency dependent ionic conductivity in  $\text{Li}_x\text{Rb}_{1-x}\text{PO}_3$  glasses has been studied using dielectric spectroscopy. The dc conductivity decreases by more than six orders of magnitude on mixing the alkali ions in the glass structure, that is, a strong mixed alkali effect on the dc conductivity was observed. The results show that the mixed alkali effect on the dc conductivity diminishes as the temperature is increased. An ac conductivity mixed alkali effect can be observed up to high frequencies, although it gradually becomes weaker as the frequency is increased. A quantitative analysis of the conductivity spectra shows that the number of mobile cations in the single alkali glasses is, within experimental uncertainty, temperature independent. The results are discussed in relation to a detailed microscopic structural model taking into account the random mixing of alkali ions [Phys. Rev. B **63**, 132202 (2001)].

DOI: 10.1103/PhysRevB.68.064202

PACS number(s): 66.30.Hs

**I. INTRODUCTION**

The intriguing mixed alkali effect (MAE) in glasses<sup>1</sup> has been an unsolved problem in glass science for several decades, and a complete understanding of the phenomenon is still lacking. The effect refers to the large deviations (several orders of magnitude) from additivity that occur in properties related to ionic transport, such as ionic conductivity and dielectric relaxation, as well as mechanical loss and internal friction, when alkali ions *A* are replaced by alkali ions *B* in glasses of the type  $A_xB_{1-x}G$ . Here, *G* may denote, for instance,  $\text{PO}_3$  in the case of metaphosphate glasses. On the other hand, other properties such as density, refractive index, thermal expansion coefficient, and elastic moduli usually exhibit only small deviations from linearity.<sup>2</sup> Properties related to structural relaxation, such as viscosity and glass transition temperature, deviates from a linear behavior, but similar deviations are also seen in mixed glass-forming systems which do not contain any cations. It should be noted that the mixed alkali effect is not unique for glasses, but is also observed in crystalline ion conductors.<sup>3</sup>

Throughout the years, several models have been proposed in order to explain the MAE.<sup>1,2,4-8</sup> These can be divided into models related to structural features, or models based on cation interactions.<sup>2</sup> The former kind of approach have attracted most attention during the last years.<sup>7</sup> One of the more recent theoretical models of ionic conduction and the MAE is the dynamic structure model (DSM).<sup>4</sup> The DSM is based on the assumption that *A* and *B* ions in a mixed alkali glass create their own local environments, which are different for different ions, leading to a site energy mismatch. The probability for an *A* ion to hop into a *B* site is lowered, compared to *A-A* or *B-B* hops, due to the site mismatch. The result is that diffusion predominantly occurs in some preferred paths, and this is proposed to account for the reduced ionic conductivity. Maass has recently used some ideas from the DSM to develop a model for the MAE without any local site relaxation.<sup>7</sup>

Recently, it was suggested that the principal features of the MAE can be qualitatively understood directly from static

structural models of real glasses.<sup>9</sup> Diffraction studies and reverse Monte Carlo (RMC) simulations of mixed alkali phosphate glasses showed that (i) the different cation species have different local and essentially composition invariant environments, and (ii) the cations are randomly dispersed between the phosphate chains in (iii) low dimensional pathways, as shown in Fig. 1. By making the assumption that the different local environments of the two kinds of alkali ions make jumps to dissimilar sites unlikely to occur (based on previous findings from, e.g., molecular-orbital calculations by Uchino *et al.*<sup>10</sup>), the MAE can be understood as a natural consequence of this structural arrangement. A static glass

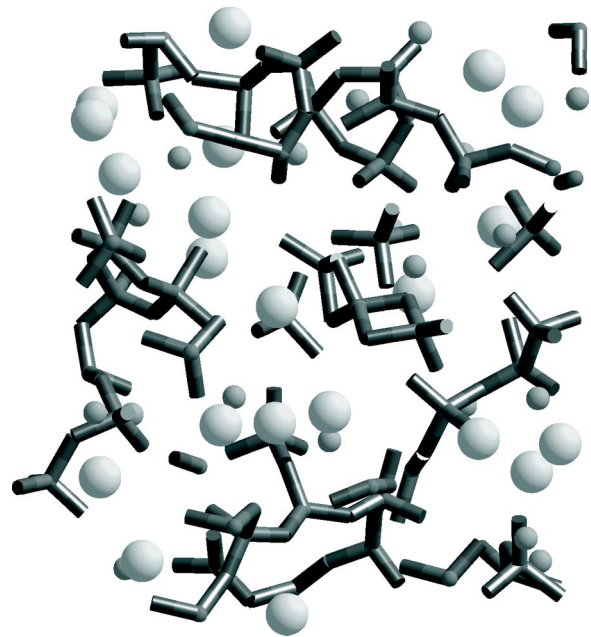


FIG. 1. A  $10 \times 10 \times 10 \text{ \AA}^3$  section of a RMC produced configuration of  $\text{Li}_{0.5}\text{Rb}_{0.5}\text{PO}_3$ . The original RMC configuration had a box length of  $42 \text{ \AA}$  and contained 5000 atoms. The phosphate network is shown as P-O bonds, small spheres are Li ions (radius  $0.6 \text{ \AA}$ ) and larger spheres are Rb ions (radius  $1.5 \text{ \AA}$ ). Note that, for clarity, the spheres representing the ions are not drawn in scale.

structure implies partial blocking of preferred diffusion paths due to the site mismatch and the random mixture of ions in low dimensional pathways. This is the essence of the random distribution model (RDM).

These different ideas have appeared separately earlier in the literature, for instance diffusion pathways,<sup>11,12</sup> a random mixing and dissimilar sites for the two types of ions.<sup>13,14</sup> Experimental support for dissimilar sites have earlier been found from vibrational spectroscopy,<sup>15</sup> extended x-ray absorption fine structure (EXAFS),<sup>14</sup> neutron diffraction,<sup>16</sup> and NMR,<sup>17</sup> while far infrared measurements,<sup>18</sup> XAFS,<sup>19</sup> and NMR<sup>20</sup> have suggested that the ions are randomly mixed. The RDM is the first model, based on real glass systems, that provides a complete structural picture of mixed alkali glasses, and which directly shows that the ions are randomly mixed in low-dimensional pathways. Furthermore, the assumptions made when the RDM was presented<sup>9</sup> have recently been confirmed<sup>21</sup> by determinations of conduction pathways in the same RMC produced structural models, using the bond-valence method.

In this paper, we have studied the conductivity in the system  $\text{Li}_x\text{Rb}_{1-x}\text{PO}_3$ , where  $x=0, 0.25, 0.5, 0.75$ , and  $1.0$ . The system is interesting for MAE studies because of the large size difference between lithium and rubidium ions. Furthermore, extensive structural characterization with Raman scattering and x-ray and neutron diffraction has been performed.<sup>22</sup> No conductivity measurements have previously been reported for this system, to our knowledge, except for the single alkali glasses  $\text{LiPO}_3$  and  $\text{RbPO}_3$ .<sup>23–25</sup> To our knowledge, the only previous conductivity MAE study on phosphate glasses is that of Chen *et al.* who investigated the  $\text{Li}_x\text{Na}_{1-x}\text{PO}_3$  system.<sup>26</sup> The present conductivity results are discussed in relation to previous structural results for the same system.<sup>22</sup> We show that the observed results are well explained using the structural random ion distribution model.<sup>9</sup>

## II. EXPERIMENT

Samples were prepared by mixing stoichiometric amounts of  $\text{Li}_2\text{CO}_3$ ,  $\text{Rb}_2\text{CO}_3$ , and  $(\text{NH}_4)_2\text{HPO}_4$ . The mixtures were held at  $900\text{--}1100^\circ\text{C}$  for 1–2 h and then poured into a circular 13-mm-diameter mould. Samples of thickness 1.5–2 mm were polished and painted with conducting silver paint to ensure good electrical contact.

Electrical conductivity measurements in the frequency range  $10^{-2}\text{--}10^6$  Hz were performed using a Novocontrol Alpha High Resolution Dielectric Analyzer. The samples were clamped between steel electrodes, of the same diameter as the sample, in the sample holder. The sample holder was placed in a nitrogen cooled cryostat during the measurements. The temperature could be controlled in the range 110–450 K with an accuracy of  $\pm 0.1$  K. Complementary measurements in the range 70–500 MHz were made at room temperature using a broadband technique which measures the complex transmission coefficient of a coaxial line including a shielded capacitorlike cell.<sup>27</sup>

From the measured sample impedance  $\hat{Z}(f) = \hat{U}/\hat{I}$ , where  $\hat{U}$  and  $\hat{I}$  are the voltage and current, respectively, expressed as complex quantities, various interrelated quantities can be

calculated. The most important are the complex relative permittivity  $\hat{\epsilon}(f) = \epsilon' - i\epsilon'' = -i/(2\pi f C_0 \hat{Z})$ , the conductivity  $\hat{\sigma}(f) = \sigma' + i\sigma'' = (\epsilon_0/C_0 \hat{Z})$ , and the modulus  $\hat{M} = 1/\hat{\epsilon}$ . In these expressions  $C_0$  denotes the empty cell capacitance,  $C_0 = \epsilon_0 A/d$ , where  $\epsilon_0$  is the vacuum permittivity,  $A$  the sample area, and  $d$  the sample thickness. According to the above definitions, the complex conductivity and permittivity are related according to  $\hat{\sigma}(f) = i2\pi f \epsilon_0 \hat{\epsilon}(f)$ .

Conductivity, or dielectric, data, can be analyzed in several ways. Ion conducting glasses are mostly analyzed within either the modulus or the conductivity formalism. There is some debate in the literature about which choice is the most correct one.<sup>28–31</sup> Here, we will use the conductivity approach. A modulus analysis of the data is presented in Ref. 32.

The real part of the frequency dependent conductivity is known empirically to follow the relation<sup>25</sup>

$$\sigma'(f) = \sigma_0 \left[ 1 + \left( \frac{f}{f_0} \right)^p \right] + Bf^{1.0}. \quad (1)$$

The first term in Eq. (1) describes a constant dc plateau. The dc conductivity  $\sigma_0$  can thus be obtained by an extrapolation of  $\sigma'(f)$  to low frequencies. The second term in Eq. (1) describes the dispersive region, which sets in approximately at the onset frequency  $f_0$ . The power law exponent  $p$  usually takes values in the range 0.5–0.7. The last term in Eq. (1),  $Bf^{1.0}$ , where  $B$  is a more or less temperature independent constant,<sup>33,34</sup> becomes important at high frequencies or at low temperatures. The origin of this term, denoted the constant loss term, is at present unclear.<sup>35,36</sup> In the frequency and temperature regions considered in this paper, the constant loss term does not play any significant role and will hence not be considered.

## III. RESULTS

Figures 2(a)–(e) show the frequency dependent conductivity  $\sigma'(f)$  for the different compositions at various temperatures. The bending of the dc plateaus at low frequencies seen in Fig. 2, clearly visible for  $\text{LiPO}_3$ , is due to polarization effects at the electrodes. These polarization effects become more significant at higher temperatures where the conductivity is high. The dc conductivity value at each temperature was taken as the conductivity  $\sigma'(f_{\text{pol}})$  at the frequency  $f_{\text{pol}}$  where polarization effects set in. The latter frequency was obtained from impedance plots where  $-Z''$  is plotted against  $Z'$ . Figure 2(f) shows an example of such an impedance plot. The intersection of the impedance arc with the  $Z'$  axis gives the dc conductivity [ $\sigma_0 = d/(Z_0 A)$ ], and also the frequency below which polarization effects dominate,  $f_{\text{pol}}$ .

The dc conductivity versus Li content in the  $\text{Li}_x\text{Rb}_{1-x}\text{PO}_3$  series is shown in Fig. 3 at two temperatures: 300 and 400 K. The points for  $x=0.5$  and  $0.75$  at 300 K in Fig. 3 were extrapolated from Arrhenius plots (to be discussed later), since no distinct dc plateaus were found in the conductivity spectra. A very clear mixed alkali effect can be observed. The drop in conductivity is six orders of magni-

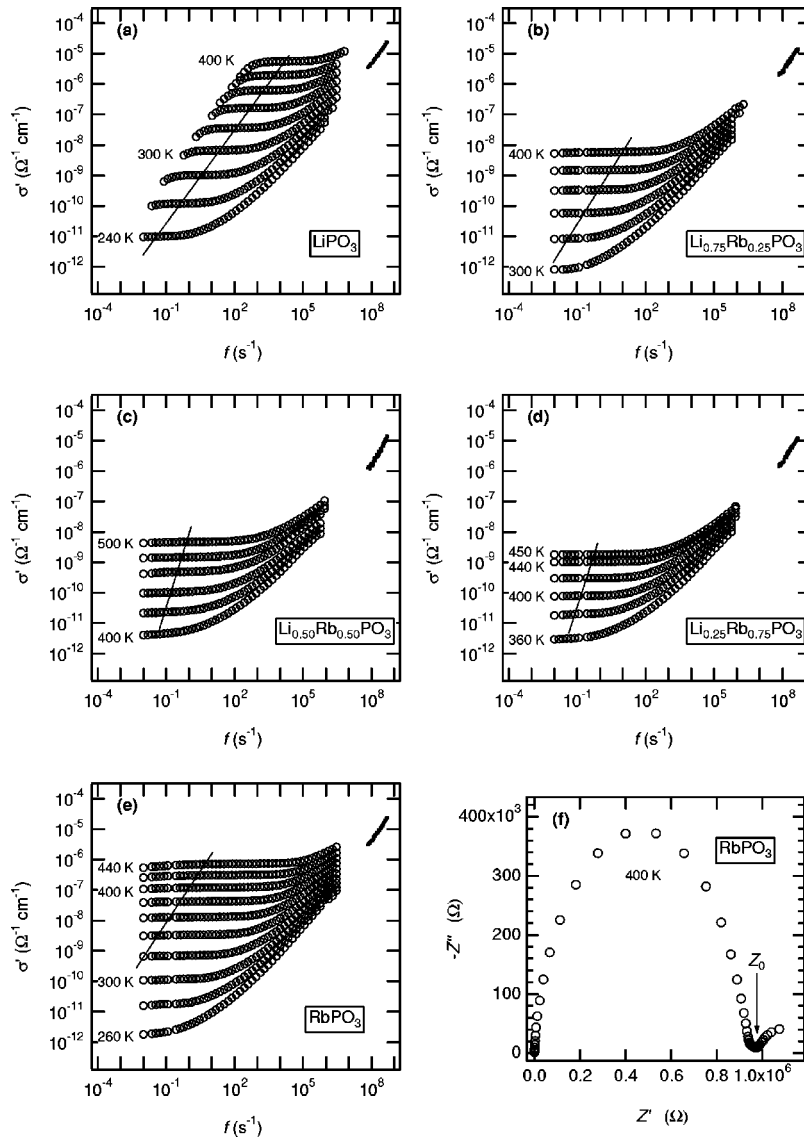


FIG. 2. Real part of the conductivity  $\sigma'(f)$  for (a)  $\text{LiPO}_3$ , (b)  $\text{Li}_{0.75}\text{Rb}_{0.25}\text{PO}_3$ , (c)  $\text{Li}_{0.5}\text{Rb}_{0.5}\text{PO}_3$ , (d)  $\text{Li}_{0.25}\text{Rb}_{0.75}\text{PO}_3$ , and (e)  $\text{RbPO}_3$  measured at various temperatures. Data points to the left of the solid lines are influenced by polarization effects. The lines intersect the conductivity curves approximately at  $f_{\text{pol}}$ . High frequency measurements (solid dots) were performed at room temperature. (f) Impedance plot of  $\text{RbPO}_3$  at 400 K. The impedance arc crosses the  $Z'$  axis at  $Z' = Z_0$ .

tude at 300 K and four orders of magnitude at 400 K. The dc conductivities obtained here for  $\text{LiPO}_3$  are slightly higher than values reported earlier.<sup>24</sup> This is probably due to different thermal histories of the samples.

In Fig. 4 the ac conductivity at room temperature (300 K) is shown at different frequencies. Although the ac mixed alkali effect is much less pronounced, it is significant, and the  $x=0.5$  sample again exhibits the lowest conductivity. This shows that there is a mixed alkali effect also at high frequencies, although the effect gradually becomes weaker. A similar behavior was reported earlier by Kulkarni *et al.*<sup>37</sup>

The dc conductivity  $\sigma_0$ , or more correctly the product of the dc conductivity and temperature,  $\sigma_0 T$ , is most oftenly found to follow an Arrhenius behavior below the glass transition temperature:

$$\sigma_0 T = A_{\sigma_0 T} \exp\left(-\frac{E_{\sigma_0 T}}{k_B T}\right), \quad (2)$$

where  $A_{\sigma_0 T}$  is a prefactor and  $E_{\sigma_0 T}$  is an activation energy. Figure 5 shows Arrhenius plots of  $\sigma_0 T$  versus inverse tem-

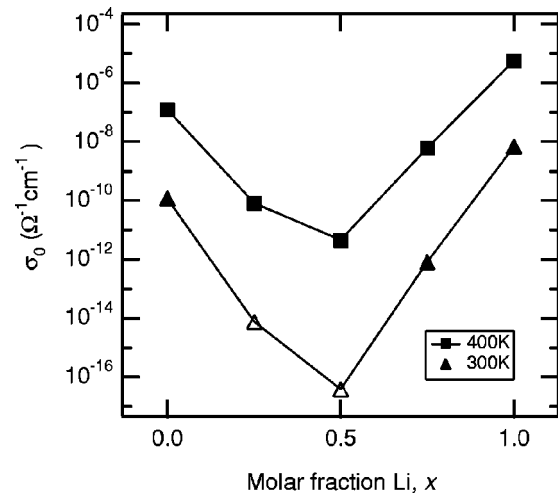


FIG. 3. dc conductivity  $\sigma_0$  vs composition for  $\text{Li}_x\text{Rb}_{1-x}\text{PO}_3$  at 300 K (filled and empty triangles) and 400 K (filled squares). The points marked with empty triangles were found from extrapolations of Arrhenius plots. The lines are guides to the eye.

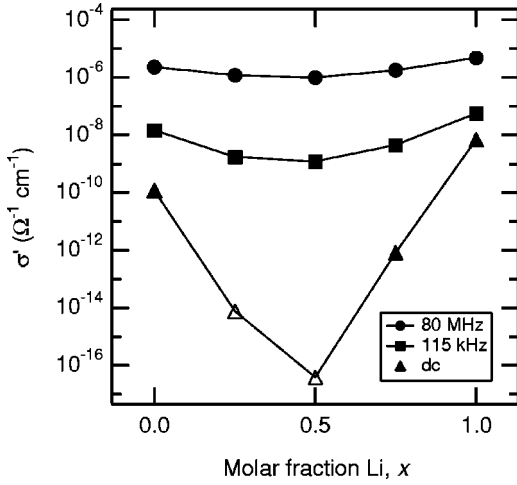


FIG. 4. Real part of the conductivity  $\sigma'$  versus composition for  $\text{Li}_x\text{Rb}_{1-x}\text{PO}_3$  in the low frequency limit (dc plateau value) (triangles), and at higher selected frequencies 115 kHz (squares) and 80 MHz (circles). All measurements at 300 K. The points marked with empty triangles were found from extrapolations of Arrhenius plots. The lines are guides to the eye.

perature for different compositions. The data were fitted to Eq. (2) and the resulting activation energies  $E_{\sigma_0 T}$  and prefactors  $A_{\sigma_0 T}$  for the different compositions are shown in Fig. 6. The activation energy goes through a maximum close to  $x=0.5$ , while the prefactor  $A_{\sigma_0 T}$  shows an increase towards a higher lithium content, with a maximum at the intermediate composition ( $x=0.5$ ).

#### IV. ANALYSIS

So far, no reference to microscopic processes has been made. One of the main problems when interpreting conductivity data is to find a connection between macroscopic measurements, such as measurements of  $\hat{\sigma}(f)$ , and microscopic processes. However, linear response theory provides a link

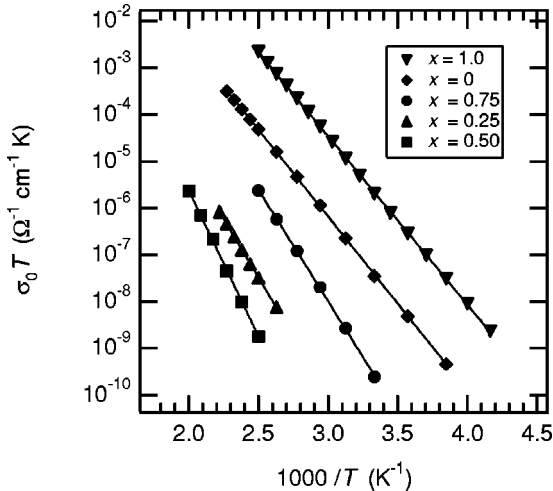


FIG. 5. Arrhenius plots of  $\sigma_0 T$  for different compositions in the  $\text{Li}_x\text{Rb}_{1-x}\text{PO}_3$  system. The full lines are fits to the data.

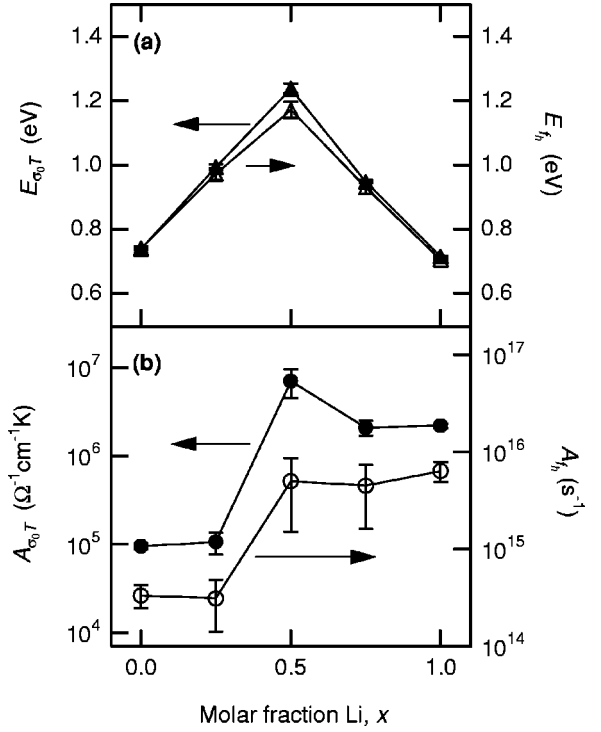


FIG. 6. (a) Prefactors and (b) activation energies obtained from curve fitting. The lines are guides for the eye.

between the mean square displacement of charge carriers,  $\langle r^2(t) \rangle$ , and the conductivity.<sup>38</sup> In Ref. 29, in which a model ion conductor is considered, it is assumed that

$$\langle r^2(t) \rangle = a^2 \left[ \left( \frac{t}{\tau} \right)^\alpha + \left( \frac{t}{\tau} \right) \right]. \quad (3)$$

Here,  $a$  is a characteristic length and  $\tau$  a characteristic time at which the mean square displacement changes from a sub-linear to a linear time dependence. That is,  $\langle r^2(t) \rangle \propto t^\alpha$ , with  $\alpha < 1$ , at  $t < \tau$  and  $\langle r^2(t) \rangle \propto t$  at  $t > \tau$ . A further assumption is that the ions move independently, that is, the Haven ratio equals one ( $H_R = 1$ ). Using linear response theory it can then be shown that the frequency dependent conductivity can be written as<sup>29</sup>

$$\sigma'(f) = \sigma_0 \left[ 1 + \left( \frac{f}{f_0} \right)^{1-\alpha} \right], \quad (4)$$

where

$$\sigma_0 = \frac{nq^2 a^2 f_h}{6k_B T} \quad (5)$$

and

$$f_0 = \frac{1}{2\pi \left[ \Gamma(1+\alpha) \cos\left(\frac{\pi}{2}(1-\alpha)\right) \right]^{1/(1-\alpha)}} f_h. \quad (6)$$

Note that Eq. (4) is Eq. (1) (with  $p=1-\alpha$ ) without any constant loss term. In Eqs. (5) and (6),  $n$  is the number density of mobile cations,  $q$  is the elementary charge,  $f_h=1/\tau$ ,

and  $\Gamma$  denotes the gamma function. Equation (5) is the familiar expression for dc conductivity, while Eq. (6) provides a link between  $f_h$  in Eq. (5) and the experimentally accessible onset frequency  $f_0$  in Eq. (1). Sidebottom *et al.* have used different arguments to arrive at essentially the same result starting from Eq. (3).<sup>39</sup>

It should be pointed out that Eqs. (4)–(6) are based on Eq. (3), which is an assumption and a simplified way to describe the ionic motion. But it is a plausible assumption, since Eq. (4) agrees with experimental data, at least in a frequency and temperature range where the influence of the constant loss term is small. Note that Eq. (3) with given values of the parameters  $a$  and  $\alpha$  is valid only for one glass composition at a time, and that  $a$  and  $\alpha$  can be expected to vary between different compositions. This is consistent with the fact that  $T$  scaling is generally observed (with one recent exception<sup>40</sup>), as long as one composition at a time is considered,<sup>41–43</sup> while  $n$  scaling, when different compositions are compared, is not.<sup>42,44–46</sup>

It still remains to give a physical interpretation of the parameters  $\tau$  and  $a$  in Eq. (3). This may be done by noting that the expression for the dc conductivity [Eq. (5)] can also be obtained from more elementary considerations,<sup>47</sup> or using linear response theory assuming random hopping.<sup>48</sup> The cations are then assumed to hop between sites with intersite spacing  $a$ , and  $f_h = 1/\tau$  is interpreted as a hopping frequency

$$f_h = A_{f_h} \exp\left(-\frac{E_{f_h}}{k_B T}\right). \quad (7)$$

In Ref. 47  $E_{f_h}$  in this expression is interpreted as an energy barrier between two sites, and  $A_{f_h}$  as a pre-exponential factor, roughly the same as the cation rattling frequency. However, in real systems these quantities are more complex.

Let us now see how the relations in Eqs. (5) and (6) can be used to make a quantitative analysis of the conductivity data. We assume that two quantities in the expression for the dc conductivity, Eq. (5), may be thermally activated: the number density  $n$  and the characteristic frequency  $f_h$  (we also assume that  $f_h$  does not depend on  $n$ ). We can then rewrite Eq. (5), with the temperature dependence of  $n$  and  $f_h$  explicitly written out, as

$$\sigma_0(T) = \frac{q^2 a^2}{6k_B T} A_n \exp\left(-\frac{E_n}{k_B T}\right) A_{f_h} \exp\left(-\frac{E_{f_h}}{k_B T}\right). \quad (8)$$

In order to investigate the activated behavior of  $n$  and  $f_h$ , Arrhenius plots of the onset frequency  $f_0$  were made, which are shown in Fig. 7. Values of  $f_0$  were obtained by fitting Eq. (4) to experimental data in the dispersion onset region with  $\sigma_0$ ,  $p$  and  $f_0$  as free parameters. Activation energies and prefactors of  $f_0$  are obtained from the Arrhenius fits, shown in Fig. 7. By using Eq. (6) (with  $\alpha = (0.30^{+0.10}_{-0.05})$ , the error limits being due to the uncertainty in the curve fitting procedure) and the activation energies and prefactors of  $f_0$ , the activation energy  $E_{f_h}$  and prefactor  $A_{f_h}$  of the hopping frequency  $f_h$  can be calculated. These are shown in Fig. 6. The activation energies  $E_{\sigma_0 T}$  and  $E_{f_h}$  are, for each composition,

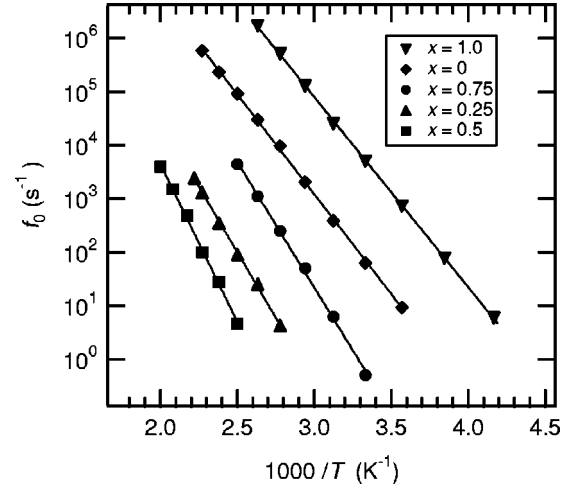


FIG. 7. Arrhenius plot of the onset frequency  $f_0$ . The full lines are fits to the data.

very similar. This implies that the temperature dependence of  $\sigma_0$  sits almost exclusively in the  $f_h$  factor, within experimental uncertainties, and that the number of conducting cations is essentially independent of temperature. There have been reports that in some glass systems  $n$  exhibits an activated behavior with activation energies  $E_n$  ranging from 0.02 eV to 0.57 eV depending on the glass composition.<sup>49</sup> We cannot detect any clear evidence of similar effects in the present glasses.

The analysis can be taken a step further in order to calculate the characteristic length (or hopping distance)  $a$ . If we assume that  $f_h$  and  $\sigma_0 T$  in Eq. (5) have the same activation energies, which just have been shown, it follows by combining Eqs. (2) and (8) (with  $E_n = 0$  and  $A_n = 1$ ) that the prefactors should be related according to

$$A_{\sigma_0 T} = \frac{nq^2 a^2}{6k_B} A_{f_h}. \quad (9)$$

By solving for the hopping distance  $a$ , we obtain

$$a = \sqrt{\frac{6k_B A_{\sigma_0 T}}{nq^2 A_{f_h}}}. \quad (10)$$

Hopping distances calculated according to Eq. (10) are shown in Table I. Values of number densities  $n$  were taken from Ref. 22. In the calculations, we have assumed that  $n$

TABLE I. Calculated hopping distances  $a$ , assuming  $c_{\text{frac}} = 1$ , and cation average nearest neighbor distances from RMC modeling. The error limits of  $a$  are estimated from errors in  $\alpha$ ,  $A_{\sigma_0 T}$  and  $A_{f_0}$ .

$x$	$a$ (Å)	$a_{\text{Li-Li}}^{\text{RMC}}$ (Å)	$a_{\text{Rb-Rb}}^{\text{RMC}}$ (Å)
0	$0.9 \pm 0.2$		$3.9 \pm 0.2$
0.25	$1.1 \pm 0.4$		
0.5	$2.6 \pm 1.1$		
0.75	$1.2 \pm 0.4$		
1.0	$0.8 \pm 0.1$	$2.9 \pm 0.1$	

$=n_{\text{majority}}$  for  $x \neq 0.5$  (that is,  $n = n_{\text{Li}}$  for  $x = 0.75$ , and vice versa), and  $n = (n_{\text{Li}} + n_{\text{Rb}})/2$  for  $x = 0.5$ . For the latter composition it is implicitly assumed that  $a_{\text{Li}} = a_{\text{Rb}} = \bar{a}$ , an average hopping distance. This means that we assume that both species may contribute to the conductivity at  $x = 0.5$ , but away from the intermediate composition only the majority carriers contribute to the conduction. Although the error limits in Table I are rather large, due to uncertain prefactor determinations, there are indications that the distance  $a$  increases in the mixed glasses. Note that the hopping distance calculations are based on the assumption that  $E_{f_h} = E_{\sigma_0 T}$ . This is not necessarily the case for  $x = 0.5$ , but even if the different activation energies are not exactly equal they are nearly equal, as can be seen in Fig. 6.

## V. DISCUSSION

### A. Single alkali glasses

The activation energies  $E_{\sigma_0 T}$  (Fig. 6) do not differ much between pure  $\text{LiPO}_3$  and  $\text{RbPO}_3$ . The dc conductivity is, however, different:  $6.4 \times 10^{-9} \Omega^{-1} \text{cm}^{-1}$  for  $\text{LiPO}_3$  and  $1.1 \times 10^{-10} \Omega^{-1} \text{cm}^{-1}$  for  $\text{RbPO}_3$  at 300 K. What matters for the different values of the conductivity is thus the prefactor  $A_{\sigma_0 T}$ , and, as has been shown above, the frequency prefactor  $A_{f_h}$ .

It has been pointed out that the activation energy  $E_{f_h}$ , or in our case equivalently  $E_{\sigma_0 T}$ , actually is the enthalpy part of a free energy<sup>50</sup>:

$$G = H - TS. \quad (11)$$

Here  $H = E_{f_h}$ ,  $T$  is the temperature and  $S$  is the activation entropy for ion migration. Since the thermally activated hopping frequency can be written as [Eqs. (5) and (8)]

$$f_h = A_{f_h} \exp\left(-\frac{E_{f_h}}{k_B T}\right) = f^* \exp\left(\frac{S}{k_B}\right) \exp\left(-\frac{H}{k_B T}\right), \quad (12)$$

we have

$$A_{f_h} = f^* \exp\left(\frac{S}{k_B}\right), \quad (13)$$

where  $f^*$  is the true attempt frequency.<sup>50</sup> This frequency should be of the same order of magnitude as the cation rattling frequency, which is of the order  $10^{12} \text{s}^{-1}$  (the cation vibration frequency is<sup>51</sup> 12 THz in  $\text{LiPO}_3$  and 3.4 THz in  $\text{RbPO}_3$ ). Hence,  $A_{f_h}$  could be considered as an effective attempt frequency, containing activation entropy contributions, in contrast to the actual attempt frequency  $f^*$ .<sup>50</sup> The differences in the prefactors of  $\text{LiPO}_3$  and  $\text{RbPO}_3$  can thus be understood as due to different activation entropies of migration.<sup>50</sup> Since  $f^*$  is of the same order of magnitudes for Li and Rb ions, Eq. (13) implies that the activation entropy is higher for  $\text{LiPO}_3$  than for  $\text{RbPO}_3$ . This result suggests that in  $\text{LiPO}_3$  there are either more mobile ions or more sites to which a Li ion can jump.

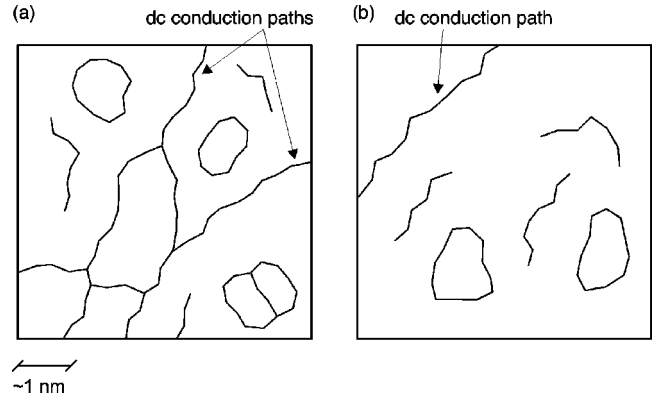


FIG. 8. Schematic illustration of conduction paths in (a) a single alkali glass ( $\text{LiPO}_3$  or  $\text{RbPO}_3$ ), and in (b) a mixed alkali glass. There are two types of conduction paths: closed and open. Only cations on the latter type contribute to the dc conductivity. The remaining cations are called trapped.

The hopping distances that we obtained (presented in Table I) are smaller than the corresponding average nearest neighbor distances (Li-Li and Rb-Rb) obtained from RMC models.<sup>9</sup> The hopping distances in Table I were calculated using Eq. (10), and assuming that all majority carriers contribute to the conductivity. Let us now instead assume that the hopping distance is roughly equal to the average nearest neighbor distances, as obtained from diffraction experiments and RMC:  $(2.8 \pm 0.2) \text{ \AA}$  for Li-Li and  $(3.9 \pm 0.2) \text{ \AA}$  for Rb-Rb.<sup>9</sup> The fraction of the cations taking part in the conduction process,  $c_{\text{frac}}$ , can then be calculated by putting  $n = c_{\text{frac}} n_{\text{tot}}$ , where  $n_{\text{tot}}$  is the total cation density, in Eq. (10). Using the numbers above, we obtain  $c_{\text{frac}} = 0.09$  for the  $\text{LiPO}_3$  glass, and  $c_{\text{frac}} = 0.05$  for  $\text{RbPO}_3$ . This indicates that of the order of 10% of the ions take part in the conduction process, provided that the hopping distances in the glasses equal the Li-Li and Rb-Rb RMC pair distances. If this is not the case, that is if the jump distances are shorter, the fraction  $c_{\text{frac}}$  would increase. However, a cation fraction of 10% is of the same order as has been found for  $\text{AgPO}_3$  glasses from bond valence pseudo potential calculations.<sup>52</sup>

So far, we have assumed the Haven ratio to be equal to one. A Haven ratio  $H_R < 1$ , which is likely to be the case for the present glasses,<sup>47</sup> would mean that  $c_{\text{frac}}$  would be even smaller, since  $H_R \neq 1$  would appear in the numerator of Eq. (10). The conclusion from this attempt to quantitative analysis, with the assumptions given above, is therefore that less than 10% of the cations in the single alkali glasses contribute to the conductivity, and that the number of conducting ions is temperature independent.

The reason why only a fraction of the cations participate in the conduction process, and that the number is independent of temperature, may be that a majority ( $>90\%$ ) of the cations are trapped, in the sense that they do not belong to conduction paths which contribute to the dc conductivity. Only the remaining, most mobile ions contribute to the dc conductivity. The trapped ions may move locally, but they do not contribute to the dc conductivity. This is illustrated schematically in Fig. 8(a).

### B. Mixed alkali glasses

The mixed alkali effect in the present Li-Rb system is very large, six orders of magnitude at 300 K. One reason for this may be the large size difference between Li and Rb ions; the difference in ionic diameter between Li and Rb is close to 2 Å.<sup>53</sup> In the  $\text{Li}_x\text{Na}_{1-x}\text{PO}_3$  system, where the diameter difference is smaller (0.8 Å), the conductivity drop is also smaller, four orders of magnitude.<sup>26</sup>

The drop in conductivity results from a drastic increase in activation energy  $E_{\sigma_0 T}$  in the mixed glasses compared to the single alkali glasses [Fig. 6(a)]. This is expected since the large size difference between Li and Rb implies a large energy mismatch between different sites. That is, a Rb ion cannot easily enter a site where a Li ion has resided, and vice versa, unless considerable structural relaxation occurs. In the mixed alkali glasses ions attempting to jump have, to varying extent, difficulties finding suitable sites. The result is, on a local level, that the rate of successful ion jumps is reduced, since ions have to climb higher energy barriers, and (consequently, since some ions get stuck), on a global level, a partial blocking of preferred diffusion pathways, such that ions are forced to diffuse along pathways with higher energy barriers than in the single alkali glasses. Both effects lead to lower conductivity and are reflected macroscopically in the increased activation energies of  $\sigma_0 T$  and  $f_h$  of the mixed glasses.

The prefactor  $A_{\sigma_0 T}$ , on the other hand as compared to the activation energy, increases when  $x$  increases from  $x=0$  to 1. The almost steplike behavior of  $A_{\sigma_0 T}$  in Fig. 6(b) may indicate that  $A_{\sigma_0 T}$  in mixed glasses is determined by the most mobile species only. This observation is consistent with the results of Ref. 32, where it was found that, with respect to the conductivity, mixed alkali glasses behave as diluted single alkali glasses. As in the single alkali glasses, the variation of  $A_{\sigma_0 T}$ , and  $A_{f_h}$  with composition may be an effect of varying activation entropy. However, the expected large reduction of the ionic degrees of freedom in the mixed glasses ought to lead to a decrease of the activation entropy, and hence a decrease of  $A_{f_h}$ , when  $x=0.5$  is approached. Our data in Fig. 6(b) do not show this, but, since the error bars are rather large, neither do the data exclude the possibility of such a decrease.

The temperature dependence of the mixed alkali effect on the dc conductivity, shown in Fig. 3, shows that the mixed alkali effect diminishes as the temperature is increased. The decrease of the MAE with temperature is a direct consequence of the higher activation energies of the mixed glasses; the average hopping rate is reduced much more rapidly as temperature decreases in mixed glasses than in single alkali glasses. The increase of the activation energy in mixed glasses can be, as discussed above, understood as primarily an effect of the partial blocking of preferred diffusion pathways, which forces the ions to move along pathways with higher energy barriers.

It is interesting to note that there is also a mixed alkali effect on the ac conductivity that remains at high frequencies, although the effect diminishes as the frequency in-

creases (Fig. 4). The latter is an effect of the fact that when the frequency increases, the typical migration distance of an ion is decreased, and hence the influence of preferred blocked pathways is reduced. Even in the mixed glass compositions most of the mobile ions will be able to find new sites in their local environments, although most of the long range preferred pathways (i.e., those contributing to the dc conductivity) are blocked by dissimilar ions and the glass network. This further implies that  $c_{\text{frac}}$  increases with increasing frequency. We note that the increase of the number of conducting ions with frequency may contribute to the increase of the slope of the  $\log \sigma'(f)$  versus  $\log f$  curve (from slope  $p \sim 0.7$  to slope 1), which is generally observed in many glass systems.

Let us now turn to a discussion on the concentration dependence of the calculated hopping distances (see Table I). The tendency towards longer hopping distances in the mixed samples could be understood as an effect of the site mismatch; when neighboring sites are energetically unfavorable, an ion has, on average, to make longer jumps in order to find a more energetically favorable position. It should be pointed out that the apparent change in jump distance when  $x$  gets closer to  $x=0.5$  could possibly also be the result of changes in the fraction of conducting ions  $c_{\text{frac}}$  when the composition is changed. However, Eq. (10) implies that in order to achieve a constant  $a$  for the various compositions,  $c_{\text{frac}}$  should be comparatively higher in the mixed compositions. This is not plausible, because of the blocking of diffusion paths. Another possible explanation for longer  $a$  in mixed compositions could be that the Haven ratio changes with  $x$ , i.e.,  $H_R$  is comparatively lower in the  $x=0.5$  composition than in the other compositions. It has, however, been found that the Haven ratio has a maximum near the intermediate composition in mixed alkali glasses.<sup>54</sup> Thus, we can rule out both these possibilities, and the analysis then suggests that there is a real increase in hopping distance upon mixing.

A schematic picture of the conduction paths in a mixed glass is shown in Fig. 8(b). The random mixture of ions hinders the formation of dc conduction paths. In the dc paths that nevertheless are formed, the average hopping distance is increased since there are less sites available. Note that the present analysis do not tell anything about  $c_{\text{frac}}$  in the mixed glasses, but it is likely to be reduced because of the blocking effect.

## VI. CONCLUSIONS

Glasses in the series  $\text{Li}_x\text{Rb}_{1-x}\text{PO}_3$  have been investigated using dielectric spectroscopy. A very strong mixed alkali effect on the dc conductivity was observed. The effect remains, although weaker, at increased temperatures ( $\sim 400$  K). A mixed alkali effect was also observed in the ac conductivity up to high frequencies.

The results can be understood within the framework of the structural random ion distribution model (RDM) where the ions are supposed to be randomly mixed between the phosphate chains. The very large mixed alkali effect observed here is then a natural consequence of the mixing of cations and the site mismatch between sites with different

species. Also the temperature dependence of the mixed alkali effect on the dc conductivity and the frequency dependence of the mixed alkali effect on the ac conductivity can be understood from the structural RDM.

An attempt to quantitative analysis based on linear response theory combined with RMC results shows that approximately 10% of the cations take part in the conduction process in the single alkali glasses. The number of conducting cations is independent of temperature within the experi-

mental accuracy. Furthermore, the analysis shows that the average ion hopping distance is longer in mixed glasses.

#### ACKNOWLEDGMENTS

This work was financially supported by the Swedish Research Council. J. S. is a Royal Swedish Academy of Sciences Research Fellow supported by a grant from the Knut and Alice Wallenberg Foundation.

- <sup>1</sup>M.D. Ingram, *Glass Sci. Technol. (Frankfurt/Main)* **67**, 151 (1994).
- <sup>2</sup>D.E. Day, *J. Non-Cryst. Solids* **21**, 343 (1976).
- <sup>3</sup>M. Meyer, V. Jaenisch, P. Maass, and A. Bunde, *Phys. Rev. Lett.* **76**, 2338 (1996).
- <sup>4</sup>A. Bunde, M.D. Ingram, and P. Maass, *J. Non-Cryst. Solids* **172-174**, 1222 (1994).
- <sup>5</sup>G.N. Greaves and K.L. Ngai, *Phys. Rev. B* **52**, 6358 (1995).
- <sup>6</sup>B.M. Schulz, M. Dubiel, and M. Schulz, *J. Non-Cryst. Solids* **241**, 149 (1999).
- <sup>7</sup>P. Maass, *J. Non-Cryst. Solids* **255**, 35 (1999).
- <sup>8</sup>R. Kirchheim, *J. Non-Cryst. Solids* **272**, 85 (2000).
- <sup>9</sup>J. Swenson, A. Matic, C. Karlsson, L. Börjesson, C. Meneghini, and W.S. Howells, *Phys. Rev. B* **63**, 132202 (2001).
- <sup>10</sup>T. Uchino, T. Sakka, Y. Ogata, and M. Iwasaki, *J. Non-Cryst. Solids* **146**, 26 (1992).
- <sup>11</sup>G.N. Greaves, *J. Non-Cryst. Solids* **71**, 203 (1985).
- <sup>12</sup>G.N. Greaves, *Philos. Mag. B* **60**, 793 (1989).
- <sup>13</sup>C.R.A. Catlow, *Phys. Status Solidi A* **46**, 191 (1978).
- <sup>14</sup>G.N. Greaves, C.R.A. Catlow, B. Vessal, J. Charnock, C.M.B. Henderson, R. Zhu, S. Qiao, Y. Wang, S.J. Gurman, and S. Houde-Walter, in *New Materials and Their Applications 1990*, edited by D. Holland, IOP Conf. Proc. No. 11 (Institute of Physics, Bristol, 1990), p. 411.
- <sup>15</sup>G.B. Rouse, P.J. Miller, and W.M. Risen, *J. Non-Cryst. Solids* **28**, 193 (1978).
- <sup>16</sup>A.C. Hannon, B. Vessal, and J.M. Parker, *J. Non-Cryst. Solids* **150**, 97 (1992).
- <sup>17</sup>R.M. Wenslow and K.T. Mueller, *J. Non-Cryst. Solids* **231**, 78 (1998).
- <sup>18</sup>E.I. Kamitsos, A.P. Patsis, and G.D. Chryssikos, *Phys. Chem. Glasses* **32**, 219 (1991).
- <sup>19</sup>G.N. Greaves, in *Defects and Disorder in Crystalline and Amorphous Solids*, edited by C.R.A. Catlow (Kluwer, Dordrecht, 1994), p. 87.
- <sup>20</sup>F. Ali, A.V. Chadwick, G.N. Greaves, M.C. Jermy, K.L. Ngai, and M.E. Smith, *Solid State Nucl. Magn. Reson.* **5**, 133 (1995).
- <sup>21</sup>J. Swenson and S. Adams, *Phys. Rev. Lett.* **90**, 155507 (2003).
- <sup>22</sup>J. Swenson, A. Matic, A. Brodin, L. Börjesson, and W.S. Howells, *Phys. Rev. B* **58**, 11 331 (1998).
- <sup>23</sup>S.W. Martin and C.A. Angell, *J. Non-Cryst. Solids* **83**, 185 (1986).
- <sup>24</sup>D.L. Sidebottom, P.F. Green, and R.K. Brow, *J. Non-Cryst. Solids* **183**, 151 (1995).
- <sup>25</sup>D.L. Sidebottom, *Phys. Rev. B* **61**, 14 507 (2000).
- <sup>26</sup>R. Chen, R. Yang, B. Durand, A. Pradel, and M. Ribes, *Solid State Ionics* **53-56**, 1194 (1992).
- <sup>27</sup>R. Pelster, *IEEE Trans. Microwave Theory Tech.* **43**, 1494 (1995).
- <sup>28</sup>K.L. Ngai and C. León, *Solid State Ionics* **125**, 81 (1999).
- <sup>29</sup>B. Roling, *J. Non-Cryst. Solids* **244**, 34 (1999).
- <sup>30</sup>D.L. Sidebottom, B. Roling, and K. Funke, *Phys. Rev. B* **63**, 024301 (2001).
- <sup>31</sup>C. León, P. Lunkenheimer, and K.L. Ngai, *Phys. Rev. B* **64**, 184304 (2001).
- <sup>32</sup>C. Karlsson, A. Mandanici, A. Matic, J. Swenson, and L. Börjesson, *J. Non-Cryst. Solids* **307-310**, 1012 (2002).
- <sup>33</sup>K.L. Ngai, *J. Chem. Phys.* **110**, 10576 (1999).
- <sup>34</sup>A.S. Nowick, A.V. Vaysleyb, and W. Liu, *Solid State Ionics* **105**, 121 (1998).
- <sup>35</sup>K. Funke and D. Wilmer, in *Solid State Ionics V*, edited by G.-A. Nazri, C. Julien, and A. Rougier, MRS Symposia Proceedings No. 548 (Materials Research Society, Warrendale, PA, 1999), p. 403.
- <sup>36</sup>C. León, A. Rivera, A. Várez, J. Sanz, J. Santamaria, and K.L. Ngai, *Phys. Rev. Lett.* **86**, 1279 (2001).
- <sup>37</sup>A.R. Kulkarni, P. Lunkenheimer, and A. Loidl, *Mater. Chem. Phys.* **63**, 93 (2000).
- <sup>38</sup>H. Scher and M. Lax, *Phys. Rev. B* **7**, 4491 (1973).
- <sup>39</sup>D.L. Sidebottom, P.F. Green, and R.K. Brow, *Phys. Rev. B* **51**, 2770 (1995).
- <sup>40</sup>S. Murugavel and B. Roling, *Phys. Rev. Lett.* **89**, 195902 (2002).
- <sup>41</sup>B. Roling, A. Happe, K. Funke, and M.D. Ingram, *Phys. Rev. Lett.* **78**, 2160 (1997).
- <sup>42</sup>B. Roling, C. Martiny, and K. Funke, *J. Non-Cryst. Solids* **249**, 201 (1999).
- <sup>43</sup>B. Roling, C. Martiny, and S. Brückner, *Phys. Rev. B* **63**, 214203 (2001).
- <sup>44</sup>B. Roling, *Solid State Ionics* **105**, 185 (1998).
- <sup>45</sup>B. Roling and C. Martiny, *Phys. Rev. Lett.* **85**, 1274 (2000).
- <sup>46</sup>Since  $f_0 \sim \sigma_0 T$  (if  $n$  is  $T$ -independent) or  $f_0 \sim \sigma_0 T/n$  (if  $n$  is Arrhenius  $T$  dependent), we can write Eq. (3) as  $\langle r^2(t) \rangle = G(D_0 T)$ , where  $G$  is some function independent of  $n$  and  $T$ , and  $D_0 = \sigma_0 k_{BT}/(nq^2)$ . However, this scaling relation, which is equivalent to a scaling relation for the conductivity,  $\sigma'(f)/\sigma_0 = F(f/D_0)$  (where  $F$  is some other scaling function) [*Phys. Chem. Chem. Phys.* **3**, 5093 (2001)], is only valid if  $a$  and  $\alpha$  are constant (that is, no temperature dependence and no composition dependence). This is usually not the case if different glass compositions are compared.
- <sup>47</sup>S.R. Elliott, *Physics of Amorphous Materials*, 2nd ed. (Longman Scientific & Technical, Harlow, 1990).
- <sup>48</sup>K. Funke, *Phys. Solid State* **22**, 111 (1993).
- <sup>49</sup>A. Pan and A. Ghosh, *Phys. Rev. B* **62**, 3190 (2000).

<sup>50</sup>D.P. Almond and A.R. West, *Solid State Ionics* **23**, 27 (1987).

<sup>51</sup>G.J. Exarhos, P.J. Miller, and W.M. Risen, Jr., *J. Chem. Phys.* **60**, 4145 (1974).

<sup>52</sup>J. Swenson and S. Adams, *Phys. Rev. B* **64**, 024204 (2001).

<sup>53</sup>R.D. Shannon, *Acta Crystallogr., Sect. A: Cryst. Phys., Diffr., Theor. Gen. Crystallogr.* **32**, 751 (1976).

<sup>54</sup>H. Jain, N.L. Peterson, and H.L. Downing, *J. Non-Cryst. Solids* **55**, 283 (1983).